nitrogen or air, and conversion curves were needed when other gases were used. Of the gases used in this work, a calibration curve was available from Granville-Phillips only for oxygen (see Figure 11). A calibration curve was constructed for *n*-butane by measuring the vapor pressure of liquid butane at different temperatures of a slush bath, employing the equation

$$\log P \text{ (torr)} = (-0.05223/T)A + B$$

where $A = 23450$ and $B = 7.395$ for butane at temperatures from −100 to +12 °C. For xenon, an indicated pressure on the GP gauge of approximately 2.2 Torr was determined to correspond to atmospheric pressure. No other calibration points were available for xenon, but a curve for krypton, in which 4.5 Torr corresponds to atmospheric pressure, was reported in the GP gauge instruction manual. Xenon was assumed to have a similarly shaped curve, but went from 2.2 rather than 4.5 Torr on the indicated pressure scale (see Figure 11). The apparent pressures of the alkylindenes in the static photolyses were also corrected, by actual measurement of the mass of "1 Torr" of 1-MI and assuming ideality of the vapor. The correction (1 Torr on the gauge = 0.67 Torr of "true" pressure) was then extrapolated to the other indenes and also assumed to be generally applicable for all low-pressure measurements in the indene series.

Quantum Efficiencies. These were carried out using, as a secondary actinometer, the reported[6] quantum efficiencies of 0.075 and 0.066, respectively, for ca. 254-nm photoisomerization of (*E*)-1-phenyl-2-butene to the *Z* isomer and cyclopropane product. Absorbance values for the actinometer and the indenes were measured in a 1-cm rectangular cell and extrapolated by the Beer-Lambert law to the cylindrical reaction vessel, after correction of the path length by the expression $L = \pi d/4$. The fraction of incident light absorbed by 1-phenyl-2-butene was quite low (3.1%) but was ca. 60% for the indenes. The experiments were typically at ca. 1 Torr, with the absolute amount of the indenes determined after correction for gauge response (see above). The amounts of the photoproducts formed were determined relative to unreacted starting material by multiple GLC analyses using column A. Light intensities were typically of the order of $(3.4-3.8) \times 10^{17}$ photons/s.

Photolyses. In flowing analytical runs, the sample (5–15 mg) was degassed at 0.02–0.05 Torr and then photolyzed by flowing through the vessel (*T* ca. 42 °C) using lamps that had been warmed up for 15 min. Typically, the pressure before the collection trap was 0.2–0.3 Torr, and the photolyses took about 1 min. Flowing preparative runs employed batches of 25–30 mg of sample, with cleaning of the quartz reaction vessel between each run to remove polymer. (The cleaning procedure utilized rinsing by acetone, hexane, acetone, and methanol; periodically a thorough baking in a glass-blower's annealing oven was required to eliminate polymer and color.) The mass recovery after photolysis was usually 75–85%. Static photolyses were carried out in an analogous fashion but with the sample constrained to the reaction vessel at the desired pressure.

Acknowledgment. We are grateful to the National Science Foundation (Grant CHE-8700333) for support of this research.

Association Dimers, Excimers, and Inclusion Complexes of Pyrene-Appended γ-Cyclodextrins

Akihiko Ueno,* Iwao Suzuki, and Tetsuo Osa

Contribution from the Pharmaceutical Institute, Tohoku University, Aobayama, Sendai 980, Japan. *Received January 17, 1989*

Abstract: Pyrene-appended γ-cyclodextrins (**1–4**) were synthesized in order to substantiate the 2:2 pyrene–γ-cyclodextrin complex as well as to determine the factors that govern their host–host and host–guest association phenomena. The absorption, circular dichroism, and fluorescence spectra of these compounds measured in 10% dimethyl sulfoxide aqueous solutions exhibit spectral characteristics of the pyrene pendant, which reflect such association phenomena. The pyrene moiety of **1** and **2** was connected with the primary hydroxyl group of γ-cyclodextrin through amide (**1**) and ester (**2**) bonds, but that of **3** and **4** was connected with the secondary hydroxyl groups at C_2 and C_3, respectively, through ester bonds. The β-cyclodextrin derivative **5**, which has a pyrene moiety connected to the primary hydroxyl group through an ester bond, was also synthesized for comparison. Compounds **1** and **2** accommodate the pyrene moiety into their own cavities, forming intramolecular inclusion complexes, which then convert into dimers with the association constants of 1.74×10^5 and 1.53×10^4 M^{-1} for **1** and **2**, respectively. However, the pyrene moiety of **3** and **4** is not deeply inserted into the cavity, resulting in the limited formation of such association dimers. The results support the reported conclusion that the 2:2 pyrene–γ-cyclodextrin complex is formed by dimerization of the 1:1 complex. The fluorescence spectra of **1–5** exhibit patterns reflecting the equilibrium between monomer and association dimer with the order of excimer to monomer intensity ratio of **5** < **4** < **3** < **2** < **1**. The observation that the ratio of **1** dropped around pH 12.5 with increasing pH led to the conclusion that in the association dimer two γ-cyclodextrin units are joined together with the secondary hydroxyl group sides facing each other. The excited pyrene moiety of **1** and **2** is remarkably protected against quenching, contrasting to the small degrees of protection of **3** and **4**. Furthermore, the pyrene excimers formed in the association dimers of **1** and **2** are almost completely protected against quenching because of isolation from the bulk water environment. Both **1** and **2** show decreased and increased intensities for excimer and monomer emissions, respectively, upon guest binding. This observation indicates that they may be used as unique sensor systems, with which guest concentration can be correlated with pyrene excimer to monomer intensity ratio.

Two-guest inclusion of γ-cyclodextrin (γ-CD, cyclooctaamylose) is of current interest in cyclodextrin chemistry[1] and presents a new aspect in host–guest chemistry since the coinclusion phenomenon has rarely been observed with other hosts. This propety of γ-CD enables it to be used as a molecular flask or container, in which two species can meet and react, and many applications might be possible on this basis as shown in some recent work, which reveals that γ-CD has remarkable promotion effects on formation of excimers,[1,2] charge-transfer complexes,[3] and photodimers of anthracene derivatives.[4] On the other hand, the

(1) Ueno, A.; Moriwaki, F.; Osa, T.; Hamada, F.; Murai, K. *J. Am. Chem. Soc.* **1988**, *110*, 4323, and references therein.

(2) (a) Ueno, A.; Takahasi, K.; Osa, T. *J. Chem. Soc., Chem. Commun.* **1980**, 921. (b) Emert, J.; Kodali, D.; Catena, R. *J. Chem. Soc., Chem. Commun.* **1981**, 758. (c) Turro, N. J.; Okubo, T.; Weed, G. C. *Photochem. Photobiol.* **1982**, *35*, 325. (d) Kobayashi, N.; Hino, Y.; Ueno, A.; Osa, T. *Bull. Chem. Soc. Jpn.* **1983**, *56*, 1849. (e) Yellin, R. A.; Eaton, D. F. *J. Phys. Chem.* **1983**, *87*, 5051. (f) Itoh, M.; Fujiwara, Y. *Bull. Chem. Soc. Jpn.* **1984**, *57*, 2261. (g) Hamai, S. *Bull. Chem. Soc. Jpn.* **1986**, *59*, 2979. (h) Eaton, D. *Tetrahedron* **1987**, *43*, 1551.

(3) Kobayashi, N.; Saito, R.; Ueno, A.; Osa, T. *Makromol. Chem.* **1983**, *184*, 837.

0002-7863/89/1511-6391$01.50/0

property of γ-CD has been used to prepare a new host series, in which two aromatic moieties are covalently linked to γ-CD and change their locations from inside to outside the γ-CD cavity upon guest binding.[5] In the case of γ-CD with one aromatic moiety, the moiety has been shown to act as a spacer, which enables the γ-CD cavity to accommodate one guest molecule by narrowing the large γ-CD cavity.[6]

It seems established that two molecules of benzene, naphthalene, and anthracene derivatives can be included into the γ-CD cavity, forming 1:2 host–guest complexes. However, in the case of pyrene, which has a much larger molecular size, several investigators reported inconsistent results.[7-12] Excimer emission from pyrene or its derivatives was markedly enhanced by γ-CD and the point of disagreement was whether the excimer was formed in a three-component (two pyrene–one γ-CD) complex (A) or a

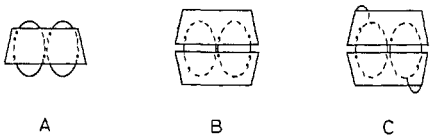

A B C

four-component (two pyrene–two γ-CD) complex (B). In the present study, we prepared pyrene-appended γ-CD's (**1–4**), together with pyrene-appended β-CD (**5**) as a reference compound, to get insight into the mechanism of the excimer formation as well as to elucidate the role of the flexible pyrene pendant in guest binding. The excimer formation and the inclusion phenomena will also be shown to be greatly affected by the nature of the bond (ester or amide) connecting the pyrene pendant to γ-CD and the site (primary or secondary hydroxyl group site) of modification.

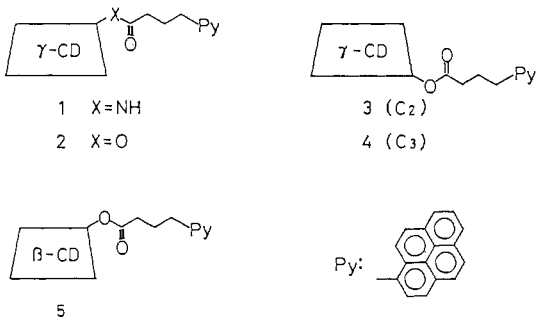

Results and Discussion

Syntheses. Cyclodextrins are doughnut-shaped molecules with the cavity having a wider face at the secondary hydroxyl group side and a narrower face at the primary hydroxyl group side. The γ-CD derivatives **1** and **2** have a pyrene moiety at the primary hydroxyl group side, while the derivatives **3** and **4** have the moiety at the secondary hydroxyl group side. The amide compound **1** was prepared by a reaction of 1-pyrenebutyric acid and 6-*O*-deoxy-6-amino-γ-cyclodextrin, which was synthesized by two-step reactions from 6-*O*-(2-naphthylsulfonyl)-γ-cyclodextrin.[13] The ester compound **2** was prepared by a reaction of 1-pyrenylbutanoyl chloride and γ-CD in pyridine at 0 °C for 2 h. The acylation of one of secondary hydroxyl groups of γ-CD was performed with *p*-nitrophenyl ester of 1-pyrenebutyric acid in an alkaline solution.[14] The reaction may proceed through complex formation between the substrate and γ-CD,[15] giving two products, which have a 1-pyrenylbutanoyl residue at C_2 and C_3 (**3** and **4**, respectively), as a mixture. These products were separable on HPLC through a reversed-phase column and identified by ^1H NMR, ^{13}C NMR, and FABMS spectra. The β-CD derivative **5** has a pyrene moiety linked to the primary hydroxyl group side through ester bond and was prepared by a reaction of 6-*O*-tosyl-β-cyclodextrin and potassium 1-pyrenylbutyrate in dimethyl sulfoxide (DMSO) at 80 °C for 5 h.

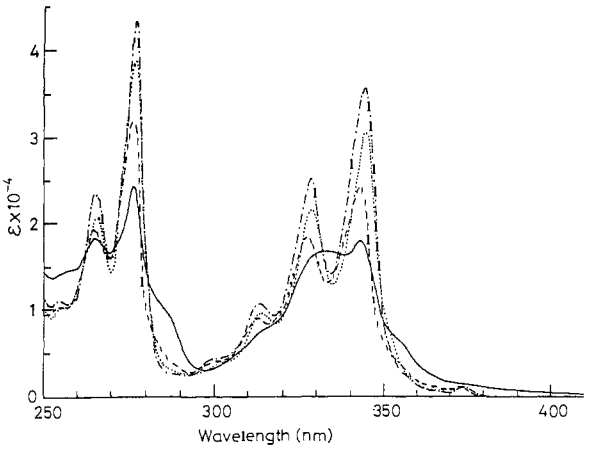

Figure 1. Absorption spectra of **1** (—), **2** (---), **3**, **4** (···), and **5** (-·-) in a 10% DMSO aqueous solution at 25 °C. The concentrations are 2.85 × 10^{-5} (**1**), 2.98 × 10^{-5} (**2**, **3**), 3.01 × 10^{-5} (**4**), and 3.00 × 10^{-5} M (**5**).

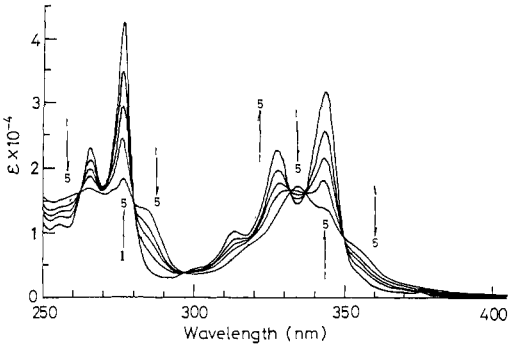

Figure 2. Absorption spectra of **1** in a 10% DMSO aqueous solution at different temperatures (1, 5 °C; 2, 25 °C; 3, 35 °C; 4, 45 °C; 5, 80 °C).

UV Spectra. Figure 1 shows absorption spectra of **1–5** in a 10% DMSO aqueous solution at 25 °C. The major electronic transitions of these substances are essentially those of pyrene itself: the typical ^1B_b and ^1L_a peaks were observed around 277 and 344 nm, respectively, with some other vibronic bands of each transition. Both **1** and **2** exhibit loss of absorption resolution and intensity due to ground-state interactions between pyrene moieties. The absorption spectrum of **1** (2.85 × 10^{-5} M) changes dramatically with temperature. Figure 2 shows absorption spectra of this solution measured at different temperatures between 5 and 80 °C. Similar spectral variations were observed for **2**. This absorption behavior may indicate diminishment of the ground-state

(4) (a) Tamaki, T.; Kokubu, T.; Ichimura, K. *Tetrahedron* **1987**, *43*, 1485. (b) Ueno, A.; Moriwaki, F.; Azuma, A.; Osa, T. *J. Chem. Soc., Chem. Commun.* **1988**, 1042.

(5) (a) Ueno, A.; Moriwaki, F.; Osa, T.; Hamada, F.; Murai, K. *Bull. Chem. Soc. Jpn.* **1986**, *59*, 465. (b) Moriwaki, F.; Ueno, A.; Osa, T.; Hamada, F.; Murai, K. *Chem. Lett.* **1986**, 1865.

(6) (a) Ueno, A.; Tomita, Y.; Osa, T. *J. Chem. Soc., Chem. Commun.* **1983**, 976. (b) Ueno, A.; Tomita, Y.; Osa, T. *Tetrahedron Lett.* **1983**, *24*, 5245. (c) Ueno, A.; Tomita, Y.; Osa, T. *Chem. Lett.* **1983**, 1635. (d) Ueno, A.; Moriwaki, F.; Tomita, Y.; Osa, T. *Chem. Lett.* **1985**, 493. (e) Ueno, A.; Moriwaki, F.; Hino, Y.; Osa, T. *J. Chem. Soc., Perkin Trans. 2* **1985**, 921.

(7) Kobashi, H.; Takahashi, M.; Muramatsu, Y.; Morita, T. *Bull. Chem. Soc. Jpn.* **1981**, *54*, 2815.

(8) (a) Kano, K.; Takenoshita, I.; Ogawa, T. *J. Phys. Chem.* **1982**, *86*, 1833. (b) Kano, K.; Matsumoto, H.; Hashimoto, S.; Sisido, M.; Imanishi, Y. *J. Am. Chem. Soc.* **1985**, *107*, 6117. (c) Kano, K.; Matsumoto, H.; Yoshimura, Y.; Hashimoto, S. *J. Am. Chem. Soc.* **1988**, *110*, 204.

(9) Harada, A.; Nozakura, G. *Polym. Bull.* **1982**, *8*, 141.

(10) Yorozu, T.; Hoshino, M.; Imamura, M. *J. Phys. Chem.* **1982**, *86*, 4426.

(11) Kobayashi, N.; Saito, R.; Hino, H.; Hino, Y.; Ueno, A.; Osa, T. *J. Chem. Soc., Perkin Trans. 2* **1983**, 1031.

(12) (a) Herkstroeter, W. G.; Martic, P. A.; Farid, S. *J. Chem. Soc., Perkin Trans. 2* **1984**, 1453. (b) Herkstroeter, W. G.; Martic, P. A.; Evans, T. R.; Farid, S. *J. Am. Chem. Soc.* **1986**, *108*, 3275.

(13) Hamada, F.; Murai, K.; Ueno, A.; Suzuki, I.; Osa, T. *Bull. Chem. Soc. Jpn.* **1988**, *61*, 3758.

(14) Ueno, A.; Breslow, R. *Tetrahedron Lett.* **1982**, *23*, 3451.

(15) VanEtten, R. L.; Sebastian, F. J.; Clowes, G. A.; Bender, M. L. *J. Am. Chem. Soc.* **1967**, *89*, 3242.

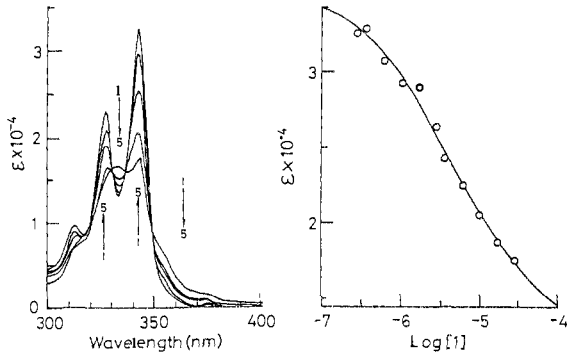

Figure 3. Absorption spectra of a 10% DMSO aqueous solution containing **1** at different concentrations at 25 °C (left: 1, 2.85×10^{-5} M; 2, 1.02×10^{-5} M; 3, 2.85×10^{-6} M; 4, 1.02×10^{-6} M; 5, 2.85×10^{-7} M) and digital simulation data of the absorption changes at 344 nm (right: solid line is the calculated curve for $K_D = 174\,000$ M^{-1}).

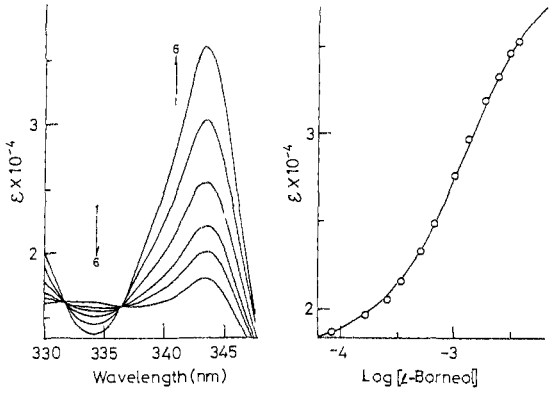

Figure 4. Absorption spectra of **1** (2.85×10^{-5} M) in a 10% DMSO aqueous solution at various *l*-borneol concentration (left: 1, 0 M; 2, 1.67×10^{-4} M; 3, 3.33×10^{-4} M; 4, 6.67×10^{-4} M; 5, 1.33×10^{-3} M; 6, 3.67×10^{-3} M) and digital simulation data of the guest-induced absorption changes at 344 nm (right: solid line is the calculated curve for $K = 2200$ M^{-1}).

pyrene–pyrene interactions at higher temperatures. Herkstroeter et al. observed similar absorption behavior in the system of γ-CD and 1-pyrenebutyric acid.[12] They concluded that a 1:1 complex first formed dimerizes to a 2:2 complex (B), in which two pyrene units are included in the cavity of the association dimer of γ-CD. Although the 1-pyrenebutyric acid unit was covalently linked to γ-CD in **1** and **2**, the associated dimers of these γ-CD derivatives (C) are likely to have the same structure as that of the native γ-CD case. The absorption spectra of **1** and **2** were markedly dependent on concentration, and the absorbance at 344 nm was used to determine the association constants. Figure 3 shows the spectra of **1** measured at different concentrations between 2.85×10^{-5} and 2.85×10^{-7} M together with the data obtained by the digital simulation method. Similar data were obtained with **2**. The analysis gave the values of 174 000 and 15 300 M^{-1} for **1** and **2**, respectively, as the association constants. The absorption coefficients at 344 nm of the monomer and the dimer were 3.51×10^4 and 1.08×10^4, respectively, for **1** and 3.30×10^4 and 9.80×10^3, respectively, for **2**. The absorption pattern of **1**, when measured at 2.85×10^{-5} M, was also dependent on the guest concentration as shown by Figure 4. The loss of the absorption resolution was canceled by guest addition, suggesting that the host–guest complexation of **1** and **2** occurs associated with dissociation of the dimer. The following two equilibria should be present in this case.

$$\mathbf{1} + \mathbf{1} \overset{K_D}{\rightleftharpoons} \mathbf{1}_2 \qquad (1)$$

$$\mathbf{1} + \text{guest} \overset{K}{\rightleftharpoons} \mathbf{1}\text{:guest} \qquad (2)$$

A digital simulation method was employed to analyze the guest-induced absorption variations of **1** and **2** (Figure 4), and the esimated host–guest association constants are shown in Table I. The binding of both **1** and **2** becomes stronger with increasing size of the guest molecules as shown by the order of cyclohexanol < *n*-octanol < *l*-menthol < *l*-borneol < 1-adamantanecarboxylic acid < cyclododecanol. It is noteworthy that **1** is a better host than **2** with larger host–guest association constants for all of these guests. The superiority of **1** in binding is particularly remarkable for larger guests such as *l*-borneol, 1-adamantanecarboxylic acid, and cyclododecanol. Since coinclusion of such large guests and the pyrene moiety seems unlikely, the pyrene moiety in the complexes probably acts as a flexible cap rather than as a spacer. On the other hand, cyclohexanol, which is the smallest among these guests, may be involved in the cavity together with the pyrene moiety. In contrast to the data of **1** and **2**, the absorptions of **3–5** were hardly affected by their concentrations or host–guest complex formation; therefore, the attachment of the pyrene moiety to the primary hydroxyl group side of γ-CD seems to be needed for the host–host association phenomenon.

Table I. Host–Guest Association Constants at 25 °C

	K, M^{-1}				
guest	**1**	**2**	**3**	**4**	**5**
cyclohexanol	13	12.5	*b*	*b*	259
n-octanol	98	63	*b*	*b*	443
l-menthol	160	118	*b*	*b*	4650
l-borneol	2200 (1800)[c]	870	13500	7800	13000
1-ACA[d]	3050 (~0)[c]	1350	23600	23600	105000
cyclododecanol	8100 (5500)[c]	4450	12400	13400	~0

[a] Values were obtained by the analyses of guest-induced UV (**1**, **2**) and circular dichroism (**3–5**) variations of the samples in 10% DMSO aqueous solutions. [b] Values too small to be measured accurately. [c] Measured in an alkaline solution (pH 13.6, 0.1 N NaOH–DMSO 9:1 by volume). [d] 1-Adamantanecarboxylic acid.

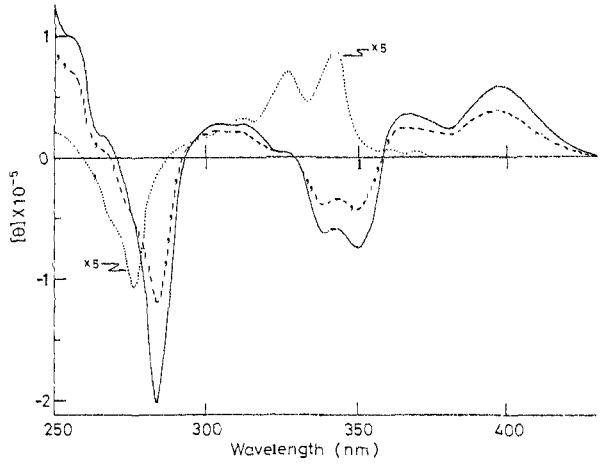

Figure 5. Circular dichroism spectra of **1** (2.85×10^{-5} M) in a 10% DMSO aqueous solution at 5 (—), 25 (---), and 80 (··) °C.

Circular Dichroism Spectra. An achiral guest molecule included in a chiral CD cavity may exhibit an induced circular dichroism (ICD) in its absorption regions. Theoretical considerations predict that the sign of the ICD is positive when a transition dipole moment of the included guest is parallel to the C_n symmetric axis of CD (axial inclusion), while the sign is negative when it is perpendicularly oriented (equatorial inclusion).[16] Pyrene shows an absorption spectrum including the ^1B_b, ^1L_a, and ^1L_b transition bands above 250 nm. It is known that the ^1B_b transition of pyrene is polarized along the short axis and the ^1L_a transition is polarized along the long axis. The 1:1 complex of pyrene and β-CD was reported to exhibit a positive ICD at the ^1L_a transition around 342 nm and a negative one at the ^1B_b transition around 278 nm.[8e] This ICD pattern substantiated that pyrene is axially included in the complex.

(16) (a) Harata, K.; Uedaira, H. *Bull. Chem. Soc. Jpn.* **1975**, *48*, 375. (b) Shimizu, H.; Kaito, A.; Hatano, M. *Bull. Chem. Soc. Jpn.* **1979**, *52*, 2678.

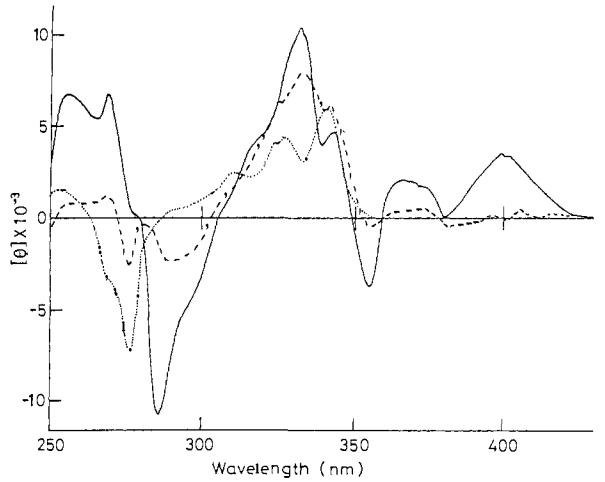

Figure 6. Circular dichroism spectra of **2** (3.03×10^{-5} M) in a 10% DMSO aqueous solution at 5 (—), 25 (---), and 65 (··) °C.

Figure 5 shows the circular dichroism spectra of **1** in a 10% DMSO aqueous solution recorded at different temperatures. The circular dichroism pattern depends markedly on temperature, and this temperature dependency should be related to the shift of the equilibrium between monomer and association dimer; the monomer and the dimer are predominant at higher and lower temperatures, respectively. The solution of **1** at 80 °C exhibits simple positive (326, 343 nm) and negative (276 nm) bands in the ^1L_a and ^1B_b transition regions, respectively. These ICD signals indicate that the monomer species forms an intramolecular complex, in which the pyrene moiety is axially included in the γ-CD cavity. By comparison, the spectrum obtained at 5 °C exhibits a complex pattern with positive signals above 350 nm (366, 397 nm), a pair of negative (338, 349 nm) and positive (290–320 nm) ones at the ^1L_a transition, and a negative one at the ^1B_b transition (284 nm). The exciton coupling theory predicts that a compound with two chromophores arranged in a left-handed chirality (S-helicity) shows a bisignated circular dichroism with negative and positive signs at the longer and the shorter wavelength regions, respectively.[17] The bisignated ICD pattern observed here in the ^1L_a transition region is very similar to that reported for the complex of pyrene and γ-CD[11] and may be attributed to the exciton coupling of S-helicity. It is noted that the positive signals above 350 nm cannot simply be attributed to the dichroism bands associated with the ^1L_b transition since the signals disappeared at higher temperatures. The detailed examination of the absorption spectra of **1** indicates that there are broad absorption bands in the corresponding region only at its high concentrations, so the absorptions and the dichroism bands appearing in the wavelength region may arise from the dimer species. The circular dichroism spectrum of **1** at 25 °C is similar to that at 5 °C with its ICD intensities slightly diminished. When measured in an alkaline solution at 25 °C, a simple ICD pattern with the characteristics of axial inclusion of the pyrene moiety was observed instead of the bisignated circular dichroism. This result implies that under alkaline conditions **1** exists as a monomer species with its pyrene moiety penetrating the γ-CD cavity to form an intramolecular complex.

Figure 6 shows the circular dichroism spectra of **2** recorded at different temperatures. The ICD pattern of **2** at 65 °C is similar to that of **1** recorded at 80 °C, exhibiting positive and negative bands in the ^1L_a and ^1B_b transitions, respectively. This result indicates that **1** and **2**, when they exist as monomer species, form similar intramolecular complexes with the pyrene moiety axially included. However, the ICD pattern becomes complicated with lowering of the temperature due to overlapping of the ICD signals of monomer and association dimer. The spectrum of **2** measured at 5 °C has an indication of bisignated Cotton effects in the ^1L_a region with negative and positive signs at the longer and shorter wavelength regions, respectively. This bisignated ICD pattern indicates that the association dimer of **2** includes two pyrene moieties with S-helicity as the dimer of **1** does. Since **1** and **2** differ only in the nature of the linking bond (amide and ester), it seems reasonable that they exhibit similar conformational features in both monomer and dimer species. It is noted, however, that **1** has a stronger tendency to insert its pyrene moiety into the γ-CD cavity, which is reflected in its greater ICD intensities.

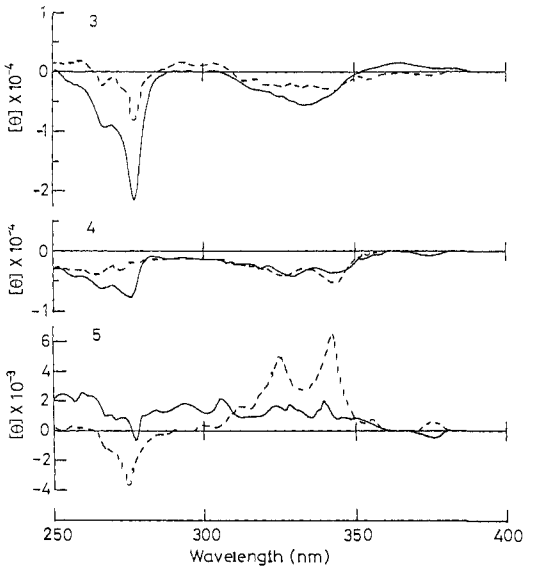

Figure 7. Circular dichroism spectra of **3–5** in a 10% DMSO aqueous solution, alone (—) or in the presence of *l*-borneol (---, 2.67×10^{-3} M) at 25 °C. The concentrations are 2.98×10^{-5} (**3**), 3.01×10^{-5} (**4**), and 3.00×10^{-5} (**5**) M.

Figure 7 shows the circular dichroism spectra of **3–5** at 25 °C. The circular dichroism spectrum of **3** exhibits simple negative bands in the ^1L_a (335 nm) and ^1B_b (276 nm) transition regions. This pattern is consistent with the equatorial inclusion and suggests that the pyrene moiety exists in the vicinity of the wider mouth of the γ-CD cavity with its long axis perpendicular to the C_8 symmetric axis of γ-CD; in other words, it does not penetrate the γ-CD cavity. The ICD intensities diminish upon addition of guests such as *l*-borneol and 1-adamantanecarboxylic acid, suggesting that **3** changes the location or orientation of the pyrene moiety in guest binding. In contrast to these guests, cyclohexanol enhanced the ICD intensities, probably due to the simultaneous inclusion of this guest with the pyrene moiety into the cavity. The ICD pattern of **4** is similar to that of **3**, suggesting that the pyrene moiety of **4** exists also in the vicinity of the wider face of the γ-CD with an equatrial orientation. Since the hydroxyl group at C-2 carbon points toward the cavity center whereas that at C-3 carbon is oriented toward the outside of the cavity, it is expected that the pyrene moiety of **3** is more likely to become close to the chiral environment of the γ-CD than that of **4**. This stereochemistry may be reflected in the fact that the dichroism intensities of **4** are smaller than those of **3**. However, the difference between **3** and **4** is not significant probably because of the flexible alkyl chain existing between the pyrene moiety and the γ-CD unit.[18] The variations of the dichroism intensity at 277 nm were used to estimate the host–guest association constants of **3** and **4**. The hosts **2–4** are regioisomers with a pyrene moiety linked to the different positions of γ-CD, and the geometrical differences might be reflected in their host–guest complexation behaviors. We found, indeed, that **3** binds *l*-borneol and 1-adamantanecarboxylic acid 16- and 17-fold more strongly than **2**, respectively. Since the binding ability of **4** is similar to that of **3**, these results suggest

(17) Harada, N.; Nakanishi, K. *Circular Dichroic Spectroscopy, Exciton Coupling in Organic Stereochemistry*; Tokyo-Kgaku-Dojin: Tokyo, 1982.

(18) Recently, we have succeeded in preparation of γ-CD derivatives, which have a 1-pyrenecarbonyl moiety in place of 1-pyrenebutanoyl at C_2 and C_3 and found marked differences in circular dichroism and fluorescence spectra between both compounds.

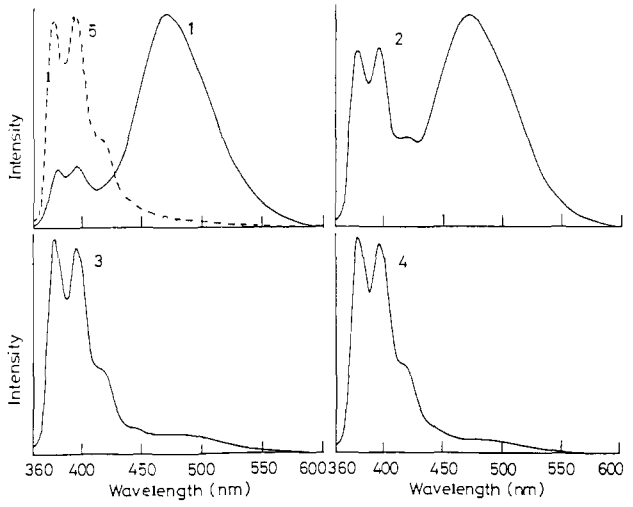

Figure 8. Fluorescence spectra of **1–5** in a 10% DMSO aqueous solution at 25 °C. The concentrations are 2.85×10^{-5} (**1**), 2.98×10^{-5} (**2**, **3**), 3.01×10^{-5} (**4**), and 3.00×10^{-5} (**5**) M.

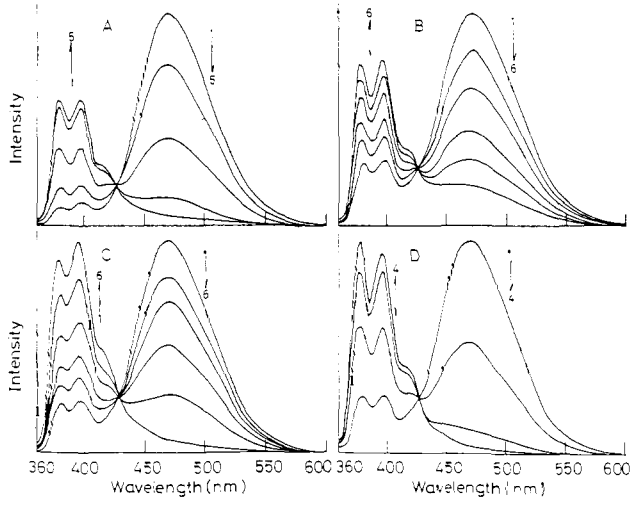

Figure 9. Fluorescence spectra of **1** (2.85×10^{-5} M) in 10% DMSO aqueous solutions at different temperatures (A: 1, 5 °C; 2, 25 °C; 3, 45 °C; 4, 65 °C; 5, 80 °C), *l*-borneol concentrations (B: 1, 0 M; 2, 3.33×10^{-4} M; 3, 6.67×10^{-4} M; 4, 1.33×10^{-3} M; 5, 2.00×10^{-3} M; 6, 3.33×10^{-3} M), pH's (C: 1, 11.32; 2, 12.24; 3, 12.48; 4, 12.72; 5, 13.02; 6, 13.48) and in solutions at different DMSO contents (D: 1, 10%; 2, 20%; 3, 30%, 4, 100%).

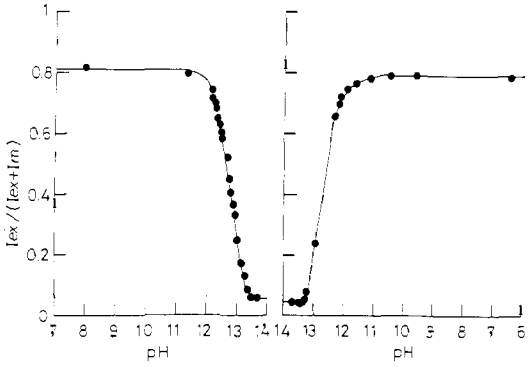

Figure 10. Intensity ratio of excimer to total emission of **1** in 10% DMSO aqueous solutions against pH (I_e and I_m are fluorescence intensities at 397 and 470 nm, respectively).

that the capping at the wider face of γ-CD is more effective in forming stable complexes. The ICD signals of **5** are weak with indication of positive sign in the ^1L_a transition region (342 nm). The weak ICD intensities of **5** agree with the conclusion led from the examination of the Corey–Pauling–Kolton (CPK) model that the bulky pyrene moiety cannot be involved fully in the β-CD cavity. Therefore, the pyrene moiety is likely to be shallowly inserted into the narrow mouth of **5** with its long axis rather parallel to the C_7 symmetric axis. It is interesting that all guests except for cyclododecanol remarkably enhanced the ICD intensities of this host. One possible explanation for this is that the hydrophobic interaction between the pyrene moiety and the included guest makes the pyrene moiety to be oriented more parallel to the C_7 symmetric axis in the complex. Table I shows host–guest association constants of **5** obtained by the analysis of the guest-induced ICD variations. The binding becomes stronger with increasing size of the guest molecules except for cyclododecanol, which is too bulky for the cavity of **5**. Table I also shows that **5** is a substantially better host for many guests compared with **1** and **2**. The strong binding of **5** may be due to its suitable cavity size. It is noted that **1** loses its binding ability for 1-adamantanecarboxylic acid in an alkaline solution. Here, the alkoxide anions of **1** prevent the anionic guest from inserting the cavity due to ionic repulsion.

Fluorescence Spectra. Figure 8 shows fluorescence spectra of **1–5** measured at 25 °C by excitation at 355 nm. The excimer fluorescence with a maximum intensity at 470 nm is seen for **1–4** with different intensity ratios to the monomer fluorescence (378, 396 nm). Since the excimers are formed by the excited-state interaction between two pyrenes, the excimer intensity ratio should be directly proportional to the concentration of the association dimers. The predominant excimer emission of **1** is consistent with the large association constant obtained by the analysis of its absorption data. The excimer emission of **2** is also remarkable with its maximum intensity comparable to that of monomer fluorescence. The excimer emission of **3** and **4** was markedly depressed, indicating that these substances exist predominantly as monomer species. The fluorescence spectrum of **5** was composed of almost pure monomer emission. These results suggest that the large cavity of γ-CD, in addition to the attachment of the pyrene moiety to the primary hydroxyl group side, is needed for excimer formation. All these fluorescence characteristics were in good agreement with the conclusion obtained from the UV and ICD spectra and confirm that the pyrene excimer can easily be formed in the association dimers of **1** and **2**. The fluorescence spectra of **1** and **2** were markedly influenced by temperature, guest, and DMSO content in solution. pH of the solution might be another factor, and its effect on the shape of fluorescence pattern was checked with **1**. Figure 9 shows the variations of the shape of the fluorescence spectrum of **1** caused by changing these factors. The excimer to monomer intensity ratio decreases with temperature. These variations are due to the dissociation of the associated dimer of **1** and coincide with the variations in the UV spectra measured with this substance. The excimer to monomer intensity ratio decreases with increasing *l*-borneol concentration. This was exactly expected from the fact that the 1:1 host–guest complex is formed at the expense of the association dimer. The ratio was found also to be dependent on the content of DMSO in the solution, decreasing with increasing content of DMSO until pure monomer fluorescence was observed at 100% DMSO. This suggests that the hydrophobic interaction, which is a main driving force for gathering the two molecules of **1** to form an association dimer, becomes lost as DMSO content increases. With regards to the pH effects, variations in the fluorescence pattern are shown in Figure 9 and the plots of the ratio of the excimer to total emission ($I_e/(I_e + I_m)$) vs pH is shown in Figure 10. The ratio of excimer to total emission is fairly uniform below pH 11.5 but drops abruptly around pH 12.5 with increasing pH. Since the pH value of the transition corresponds to the pK_a of the secondary hydroxyl groups of CD,[19] the diminishment in the excimer intensity ratio caused by increasing pH may be related to the formation of anionic forms of the secondary hydroxyl groups of **1**. This pH dependency suggests that the secondary hydroxyl group sides of

(19) VanEtten, R. L.; Clowes, G. A.; Sebastian, J. F.; Bender, M. L. *J. Am. Chem. Soc.* **1967**, *89*, 3253.

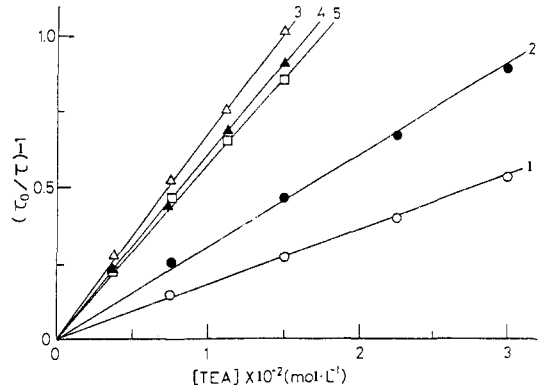

Figure 11. Stern–Volmer plots of **1–5** in a 10% DMSO aqueous solution obtained at 25 °C by using TEA as the quencher.

1 are faced with each other in the association dimer (C) and the dimer is dissociated into two monomer species above pH 13.5 due to the ionic repulsion between the two negatively charged faces. This argument was confirmed by the fact that the excimer emission appeared again at exactly the same pH as it disappeared when the pH of the solution was lowered by hydrochloric acid (1 M) from 14.

Fluorescence Quenching. With regards to the location of the pyrene moiety of **1–5**, the ICD studies have shown different degrees of insertion of the moiety into the CD cavities. Quenching of the fluorescence of the pyrene moiety by an appropriate hydrophilic quencher (Q) would also allow us to evaluate the extent of insertion since the access to the pyrene moiety should be hindered if the moiety is involved into the CD cavities. We chose triethanolamine (TEA) for this purpose, as Herkstroeter et al. did for the system of γ-CD and 1-pyrenebutyric acid.[12]

The decay curves for monomer fluorescence of **1–5** in a 10% DMSO aqueous solution as well as in DMSO were best fitted with two exponentials; one component makes a large contribution (>99%) to the total of the monomer fluorescence and another component is present as a minor species. Since the minor species exists only as traces, it seems not practical to identify it or to make any kinetical treatment for it. We therefore describe here the results of fluorescence measurements only for the major species. The quenching rate constants k_q may be determined from the following Stern–Volmer equation

$$I_0/I = \tau_0/\tau = 1 + K_{SV}[Q] = 1 + k_q\tau_0[Q]$$

where K_{SV} and k_q are Stern–Volmer and quenching rate constants, respectively, and the subscript 0 denotes the absence of quencher. Figure 11 shows the plots for the quenching of monomer fluorescnece of **1–5** in a 10% DMSO aqueous solution. The k_q values obtained under various conditions are summarized in Table II. The k_q values in a 10% DMSO aqueous solution indicate that the protection by the CD walls increases in the order **3** < **4** < **5** < **2** < **1**. Among the four γ-CD derivatives, the pyrene moiety of **1** and **2** is substantially more protected than that of **3** and **4**. The higher degrees of protection observed for **1** and **2** may be due to the smaller polarity of the primary hydroxyl side of the CD unit in comparison with the polar secondary hydroxyl side. This argument means that the narrower face of the primary hydroxyl group side of γ-CD is more effective to catch and bind the pyrene moiety than the wider face of the secondary hydroxyl group side. Consequently, the pyrene moiety of **3** and **4** is protected in smaller degrees even in comparison with that of **5**. All these results agree with the conclusion drawn from the ICD data. Addition of *l*-borneol to the 10% DMSO aqueous solutions of **1** and **2** caused remarkable increases in the k_q values. This canceling of protection suggests that the pyrene moiety moves to the exterior of the γ-CD cavity when **1** and **2** bind the guest. In the complexes, the pyrene moiety is likely to contact with the included guest as a cap, while surrounded partly by the bulk water environment. Because of this structure of the complexes of **1** and **2**, the quenching by TEA is still limited. In contrast to the cases of **1** and **2**, addition of *l*-borneol to the solutions of **3** and **4** resulted in considerable decreases in the k_q values. This result means that the guest molecule hinders the access of TEA to the pyrene moiety of **3** and **4**. The possible explanation for this is that the pyrene moiety, which exists in the vicinity of the wider mouth of **3** and **4**, becomes more deeply involved into the cavity associated with the guest accommodation. On the other hand, **5** exhibited the increased k_q value in the presence of *l*-borneol, indicating that the pyrene moiety of **5** is more surrounded by the bulk water environment in the complexes. Table II also shows the data obtained for quenching of the monomer fluorescence of **1** in an alkaline solution. Under the conditions, the canceling of the protection was observed in the presence of *l*-borneol to the similar degree as seen for **1** in a 10% DMSO aqueous solution. DMSO is the solvent, in which usual hydrophobic interactions are unlikely or weak[20,21] and access to the pyrene moiety by TEA would be fully allowed. From this viewpoint, the use of DMSO as a solvent might be expected to make **1–4** not distinguishable in quenching by TEA. We found, however, that in DMSO there still remain different degrees of quenching among these pyrene-appended CD's. The considerable degree of protection against quenching observed for **1** indicates that this substance has a tendency to insert the pyrene moiety into its own γ-CD cavity even in the solution without water. This argument was substantiated by the fact that **1** exhibits circular dichroism bands even in DMSO. The substances **2–4** gave similar k_q values, which are greater than that of **1** but slightly smaller than that of **5**; therefore the protection against quenchign occurs, although to lesser extents in comparison with the case of **1**, for these γ-CD derivatives in DMSO.

Table II. Quenching Rate Constants for Pyrene-Appended CD's at 25 °C[a]

fluorophore	condition	τ_0, ns	k_q, M^{-1} s^{-1}
1	10% DMSO	152	1.16×10^8
	10% DMSO, *l*-borneol[b]	172	3.73×10^8
	10% DMSO, pH 13.6[c]	154	1.43×10^8
	10% DMSO, pH 13.6,[b] *l*-borneol[c]	165	3.44×10^8
	DMSO	123	5.68×10^8
	10% DMSO (excimer)[d]	117	3.93×10^6
2	10% DMSO	166	1.78×10^8
	10% DMSO, *l*-borneol[b]	172	4.23×10^8
	DMSO	130	8.69×10^8
	10% DMSO (excimer)[d]	114	1.17×10^7
3	10% DMSO	138	4.91×10^8
	10% DMSO, *l*-borneol[b]	156	3.08×10^8
	DMSO	124	8.71×10^8
4	10% DMSO	134	4.51×10^8
	10% DMSO, *l*-borneol[b]	140	3.33×10^8
	DMSO	119	8.82×10^8
5	10% DMSO	149	3.88×10^8
	10% DMSO, *l*-borneol[b]	155	5.25×10^8
	DMSO	129	9.69×10^8

[a] These k_q values were obtained from measurements of lifetimes in argon-purged solutions. TEA was used as the quencher. [b] Measured for the solution containing *l*-borneol (2.67×10^{-3} M). [c] 0.1 N NaOH–DMSO 9:1 by volume. [d] Measured at 500 nm.

The excimer fluorescence of **1** and **2** in an aqueous 10% solution was also quenched by TEA, but the k_q values are substantially small (Table II). These data indicate that the excimers formed in the association dimers of these substances are markedly protected from quenching by TEA. It means that the pair of pyrenes in the association dimers is almost completely isolated from the bulk water environment. This phenomenon is exactly the same as reported by Herkstroeter in the system of native γ-CD and 1-pyrenebutyric acid.

Conclusions

The γ-CD derivatives **1** and **2** exhibit a marked tendency to form an association dimer, in which two pyrene moieties form an excimer. The structural difference between **1** and **2** resides only

(20) Siegel, B.; Breslow, R. *J. Am. Chem. Soc.* **1975**, *97*, 6869.
(21) Ueno, A.; Moriwaki, F.; Matsue, T.; Osa, T.; Hamada, F.; Murai, K. *Makromol. Chem., Rapid Commun.* **1985**, *6*, 231.

in the nature of the bond between 1-pyrenylbutanoyl residue and γ-CD unit, amide, and ester bonds for **1** and **2**, respectively, but **1** gave much greater host–host and host–guest association constants than those of **2**, demonstrating the importance of the connecting bond used for modification of γ-CD. The pyrene moiety of **3** and **4** are likely to be located in the vicinity of the wider mouth with small degrees of insertion into the γ-CD cavity. This structural feature of **3** and **4** was reflected in their binding abilities as shown by the fact that **3** and **4** are better hosts than **1** and **2**, which have the pyrene moiety at the narrower mouth of γ-CD. Consequently, it was substantiated that the capping of the cavity from the wider face is very effective in converting γ-CD to a series of hosts with strong binding abilities. The limited formation of the association dimer of **3** and **4** demonstrates that the association dimers of **1** and **2** are formed via intramolecular self-complexation forms. This way for formation of association dimers may be related to the reported conclusion that the 2:2 host–guest complex of pyrene and γ-CD is formed by dimerization of the 1:1 complex. The excimers formed in the association dimers of **1** and **2** were markedly protected against quenching, confirming that the included pyrene moieties are isolated from the bulk water environment. The association dimers of **1** and **2** dissociate into the 1:1 host–guest complexes upon guest addition, resulting in increase and decrease of monomer and excimer emission intensities, respectively. These systems may be useful as unique sensors for detecting various guest substances as variation of pyrene excimer to monomer fluorescence ratio.

Experimental Section

Measurements. NMR spectra were recorded on JEOL JNM-GX 500 and JNM-FX 100 spectrometers. FABMS spectra were obtained with a JEOL DX303 instrument. HPLC separation was performed on a Jasco 800 series. The circular dichroism spectra were recorded on a Jasco J-400X spectrodichrometer. UV spectra were measured on a Shimadzu UV-250 spectrophotometer using cells with 5-, 10-, and 50-mm pass lengths. Fluorescence spectra were recorded on a Schimadzu RF-500 spectrofluorophotometer by excitation at 355 nm. Fluorescence decay curves were obtained at 25 °C by a Horiba NAES-550 series, using a combination of a glass (HOYA u-360) and a solution (K_2CrO_4, 0.27 g L^{-1}, 1 cm) for excitation around 320 nm and a monochrometer for monitoring the emission at 378 or 500 nm. All solutions for fluorescence decay measurements were purged with argon before measurement.

6-Deoxy-6-amino-[4-(1-pyrenyl)butanoyl]-γ-cyclodextrin (1). A solution of 4-(1-pyrene)butyric acid (250 mg, 0.9 mmol) and *N,N*-dicyclohexylcarbodiimide (206 mg, 1.0 mmol) in DMF was stirred at −4 °C for 40 min. To the mixture was added 6-deoxy-6-amino-γ-cyclodextrin (259 mg, 0.2 mmol)[13] and the resultant solution was stirred at the same temperature for another 30 min and then at room temperature for 5 h. After filtration, the reaction mixture was poured into acetone (250 mL) and the precipitate was collected. Sephadex LH-20 column chromatography (25 × 1000 mm) with a mixture of DMF and water (35:65 by volume) afforded the fractions that contain the desired product. The fractions were concentrated and poured into acetone, and the precipitate was collected, washed with acetone and ether, and dried in vacuo at 80 °C (61.3 mg, 18%): R_f 0.56 (*n*-butanol–ethanol–water 5:4:3); MS (FAB) *m/e* 1566 (M^+); IR (KBr) 1550 cm^{-1}; ^1H NMR (DMSO-d_6); 500 MHz) δ 1.95–2.05 (2 H, m), 2.20–2.35 (2 H, m), 3.10–3.80 (m), 4.35–4.65 (7 H, m), 4.80–4.95 (8 H, m), 5.60–5.90 (16 H, m), 7.68 (1 H, s), 7.90–8.40 (9 H, m). Anal. Calcd for $C_{68}H_{95}O_{40}N\cdot 9H_2O$: C, 47.25; H, 6.59; N, 0.81. Found: C, 47.01; H, 6.17; N, 0.93.

6-*O*-4-[(1-Pyrenyl)butanoyl]-γ-cyclodextrin (2). A solution of γ-CD (1.32 g, 1 mmol) and 4-(1-pyrenyl)butanoyl chloride (0.387 g, 1.2 mmol) in pyridine was stirred at 0 °C for 2 h. The reaction mixture was concentrated to 10 mL under reduced pressure and poured into acetone (200 mL), and the precipitate was collected. Sephadex LH-20 column chromatography (25 × 1000 mm) with a mixture of DMF and water (1:1 by volume) afforded the fractions that contained the desired product. The fractions were concentrted under reduced pressure and poured into acetone to yield the precipitate. Crystallization from a mixture of ethylene glycol and water afforded pale orange powder (114 mg, 7%): R_f 0.55 (*n*-butanol–ethanol–water 5:4:3); MS (FAB) *m/e* 1567 (M^+); IR (KBr) 1725 cm^{-1}; ^1H NMR (DMSO-d_6; 100 MHz; 60 °C) δ 1.8–2.2 (2 H, m), 2.7–4.0 (m), 4.1–4.7 (7 H, m), 4.7–5.1 (8 H, m), 5.5–6.1 (16 H, m), 7.8–8.5 (9 H, m); ^{13}C NMR (DMSO-d_6) δ 26.65, 31.83, 32.97 (methylene C), 59.53–60.07 (C_6), 62.77 (C_6'), 69.01 (C_5'), 72.13–72.92 (C_2, C_3, C_5), 80.28–81.96 (C_4), 101.53–101.77 (C_1), 102.52 (C_1'), 123.39–130.86 (pyrene C_2–C_{16}), 136.22 (pyrene C_1), 172.77 (carbonyl C). Anal. Calcd for $C_{68}H_{94}O_{41}\cdot 7H_2O$: C, 48.23; H, 6.43. Found: C, 48.09; H, 6.03.

4-Nitrophenyl 4-(1-Pyrenyl)butanoate. A solution of 4-(1-pyrene)-butyric acid (1.32 g, 4.58 mmol), *N,N*-dicyclohexylcarbodiimide (1.04 g, 5.04 mmol), and 4-(*N,N*-dimethylamino)pyridine in methylene chloride (150 mL) was stirred at room temperature until the solution became clear. After addition of 4-nitrophenol (0.615 g, 5.04 mmol) in ether (10 mL), the solution was stirred for 5 h. Evaporation of the solvent followed by column chromatography on silica gel with a mixture of *n*-hexane and methylene chloride (1:1 by volume) afforded the product (0.55 g, 29%): R_f 0.28 (*n*-hexane–methylene chloride 1:1); IR (KBr) 1780 cm^{-1}; ^1H NMR ($CDCl_3$; 100 MHz) δ 2.20 (2 H, q, *J* = 7 Hz), 2.65 (2 H, t, *J* = 7 HZ), 3.35 (2 H, t, *J* = 7 Hz), 6.9–7.1 (2 H, m), 7.7–8.1 (9 H, m).

2-*O*-4-[(1-Pyrenyl)butanoyl]-γ-cyclodextrin (3), 3-*O*-4-[(1-Pyrenyl)-butanoyl]-γ-cyclodextrin (4). A carbonate buffer solution (2 mL, pH 10.6) was added to the mixture of DMF (2 mL), γ-CD (65 mg, 0.05 mmol), and 4-nitrophenyl 4-(1-pyrenyl)butanoate (20.5 mg, 0.05 mmol). The resultant solution was stirred for 15 min at room temperature, neutralized with HCl (0.1 N), and evaporated under reduced pressure. To the solid residue was added water (2 mL), and the insoluble materials were removed by filtration. Column chromatography on Biobeads SM-4 (30 × 300 mm) with water (300 mL), methanol–water (1:1 by volume, 100 mL), and ethanol–water (3:1 by volume, 100 mL) as the solvents afforded the fractions that contained the crude product. Purification by column chromatography on Sephadex LH-20 (25 × 1000 mm) with a mixture of DMF and water (1:1 by volume) gave the fractions that contained **3** and **4**. The fractions were concentrated under reduced pressure and poured into acetone to give white powder (55 mg, 65%). The 30% dimethylformamide aqueous solution containing **3** and **4** as the mixture was injected into a HPLC column (YMC S-343-15, ODS, 20 × 250 mm), and the absorption at 344 nm was monitored while a gradient elution (30% MeOH–80% MeOH) was applied. The regioisomers **3** and **4** were separable on the column, showing maximal absorptions at 39 and 50 min, respectively, after the injection. After the removal of methanol under reduced pressure, the collected fractions were lyophilized to give the desired products (56:44 for **3** and **4**). **3**: MS (FAB) *m/e* 1567 (M^+); IR (KBr) 1720 cm^{-1}; ^1H NMR (DMSO-d_6; 500 MHz) δ 2.07 (t, *J* = 7.0 Hz, 2 H, CH_2), 2.56–2.69 (m, 2 H, CH_2), 3.19–3.79 (m), 3.94 (t, *J* = 7.0 Hz, 1 H, $C_3'H$), 4.42–4.67 (m, 9 H, O_6H, $C_2'H$), 4.75 (t, *J* = 4.0 Hz, 1 H, $C_1'H$), 4.84–5.00 (m, 7 H, C_1H), 5.29–6.09 (m, 13 H, O_2, O_3H), 8.00–8.53 (m, 9 H, aromatic); ^{13}C NMR (DMSO-d_6) δ 26.67, 32.15, 33.24 (CH_2), 59.53–60.43 (C_6), 69.38 (C_3'), 71.79–73.27 (C_2, C_3, C_5), 73.80 (C_2'), 78.43 (C_4'), 79.62–81.54 (C_4), 97.44 (C_1'), 100.76–101.98 (C_1), 123.65–130.90 (pyrene C_2–C_{16}), 136.63 (pyrene C_1), 172.61 (C=O). Anal. Calcd for $C_{68}H_{94}O_{41}\cdot 8H_2O$: C, 47.72; H, 6.48. Found: C, 47.89; H, 6.70. **4**: MS (FAB) *m/e* 1567 (M^+); IR (KBr) 1720 cm^{-1}; ^1H NMR (DMSO-d_6; 500 MHz) δ 1.98–2.13 (m, 2 H, CH_2), 2.41–2.66 (m, 2 H, CH_2), 3.12–3.81 (m), 4.43–4.65 (m, 8 H, O_6H), 4.75 (d, *J* = 6.0 Hz, 1 H, $O_2'H$), 4.82–4.99 (m, 8 H, C_1H), 5.19–5.89 (m, 15 H, O_3H), 7.96–8.46 (m, 9 H, aromatic); ^{13}C NMR (DMSO-d_6) δ 26.62, 32.00, 33.70 (CH_2), 59.83–59.96 (C_6), 71.07 (C_2'), 71.10–73.00 (C_2, C_3, C_5), 73.70 (C_3'), 77.13 (C_4'), 80.35–81.04 (C_4), 101.20–101.75 (C_1), 123.59–130.88 (pyrene C_2–C_{16}), 136.72 (pyrene C_1), 172.36 (C=O). Anal. Calcd for $C_{68}H_{94}O_{41}\cdot 9H_2O$: C, 47.22; H, 6.53. Found: C, 47.10; H, 6.49.

6-*O*-4-(1-Pyrenyl)butanoyl-β-cyclodextrin (5). A solution of 6-*O*-tosyl-β-cyclodextrin (516 mg, 0.4 mmol) and potassium 1-pyrenylbutanoate (144 mg, 0.44 mmol) in DMSO (8 mL) was stirred at 80 °C for 5.5 h. After cooling, the reaction mixture was poured into acetone (200 mL), and the precipitate was collected. Column chromatography on Sephadex LH-20 gel with a mixture of DMF and water (1:1) gave the fractions that contained the crude product. The fractions were concentrated under reduced pressure and poured into acetone to yield the precipitate. Recrystallization from a mixture of *n*-butanol–ethanol–water (5:4:3 by volume) and acetonitrile gave the product as pale brown powder (184 mg, 31%): R_f 0.56 (*n*-butanol–ethanol–water 5:4:3); MS (FAB) *m/e* 1405 (M^+); IR (KBr) 1725 cm^{-1}; ^1H NMR (DMSO-d_6; 100 MHz) δ 1.8–2.2 (2 H, m), 3.0–4.0 (m), 4.1–4.7 (6 H, m), 4.8–5.0 (7 H, m), 5.5–6.0 (14 H, m), 7.8–8.5 (9 H, m). Anal. Calcd for $C_{62}H_{84}O_{36}\cdot 5H_2O$: C, 49.80; H, 6.34. Found: C, 49.53; H, 6.00.

Acknowledgment. We express our gratitude to Dr. K. Itaya for his generosity and help in performing fluorescence lifetime measurements on the NAES-550 instrument. This work was supported by Grants-in-Aid 61470152 and 61550585 from the Ministry of Education, Science and Culture.